euspen's 26th International Conference & Exhibition, Krakow, PL, June 2026
www.euspen.eu

Development of an innovative process chain to enhance the durability of functionalized polymer surfaces for real-world applications.

G. Baruffa[1]; G. Lucchetta[1]; M. Sorgato[1]

[1]Department of Industrial Engineering, University of Padova, via Venezia 1, Padova, 35131, Italy

giacomo.baruffa@studenti.unipd.it

Abstract
Surface engineering enhances injection-molded polymers components via micro- and nanometric features, but the poor durability of these nanostructures limits their real-world application. Two methods can boost robustness: self-protective surfaces, in which micrometric features shield nanopatterns from mechanical stress, and self-recovering surfaces, made from elastic materials that can rebound after deformation. This work demonstrates an IM-based process chain using micro-injection molding (μ-IM) to manufacture touch-resistant functionalized surfaces. Self-protective surfaces result from superimposing micrometric protective grids onto laser-induced periodic surface structures (LIPSS) responsible for structural coloration. Surface replication was studied using a rigid thermoplastic (PP) and a thermoplastic elastomer (SEBS). The effects of molding parameters on replication accuracy and uniformity at micro- and nanoscales were systematically examined. The results reveal markedly different replication mechanisms for the two materials. For PP, replication uniformity is primarily governed by the distribution of packing pressure and the hesitation effect. In contrast, SEBS replication is dominated by shear-induced macromolecular relaxation, which affects both replication accuracy and uniformity. Abrasion tests confirm that both strategies enhance surface durability; the self-recovering approach is more effective but more challenging to apply. Overall, this study provides new insights into the replication behavior of thermoplastic elastomers in μ-IM and establishes practical guidelines for industrial implementation of durable, nanostructured polymer surfaces.

Keywords: Molding (or moulding); Polymer; Wear; Microstructure

1. Introduction

Injection molding (IM) is widely used for the large-scale production of polymer components with micro- and nanoscale surface features [1]. However, nanofeature durability is limited by their small size and low mechanical properties of polymers, making the nanotexture sensitive to minimal stresses, such as the human touch [2]. A common mitigation strategy, known as self-protective surfaces, employs hierarchical architectures in which microscale features absorb most mechanical loads, thereby protecting the functional nanofeatures [3]. In this case, durability depends on the integrity of the microfeatures, which may degrade under repeated loading. The use of elastomers improves surface durability by enabling self-recovery of shape after load removal [2,4]. Thus, thermoplastic elastomers (TPEs) are suitable for combining self-recovering surfaces with IM.

Integrating nano-scale features into IM components requires defining a process chain to produce the nanotextures on the mold surface and accurately replicate them during molding [1].

Accurate replication is crucial for surface functionality, as poor replication can impair performance. Processing parameters significantly affect replication quality [5]. In the case of rigid thermoplastic materials, high mold and melt temperatures, raised injection speeds, and increased packing pressures are commonly reported as effective strategies to enhance replication accuracy [5,6]. Moreover, several studies have demonstrated that the replication quality is also affected by the distance between the gate and the features [6,7]. Conversely, the effect of IM process parameters on the replication accuracy of TPEs has been significantly less explored. TPEs are phase-separated materials, composed of a hard crystalline phase and a soft elastomeric phase, which respond differently to molding conditions. As with rigid thermoplastics, raised packing pressures and higher mold temperatures generally improve replication accuracy; however, these conditions may also lead to surface defects [8]. The influence of injection speed remains poorly understood, with some studies reporting adverse effects on replication accuracy [9]. Moreover, results have differed regarding the impact of melt temperature on replication accuracy [9,10]. To the best of the authors' knowledge, the replication uniformity of TPEs has not yet been fully studied.

This study demonstrates the feasibility of combining self-protective and self-recovering strategies within a single μ-IM process chain to manufacture touch-resistant diffractive gratings for structural coloration. Surfaces were replicated using a rigid thermoplastic (polypropylene, PP) and a thermoplastic elastomer (styrene–ethylene–butylene–styrene, SEBS). By systematically investigating the distinct replication mechanisms of these two materials and evaluating durability through abrasion tests, the effectiveness of the proposed approach was confirmed. Overall, this work provides new insights into TPE replication in μ-IM and establishes a practical framework for integrating robust nanofeatures into injection-molded components, offering comprehensive process and design guidelines for real-world applications.

2. Materials and methods

2.1. Micro injection molding

In this study, three previously developed self-protective surfaces were considered [11]. The surfaces, textured through ps-laser machining, consist of a diffractive grating based on infrared Laser-Induced Periodic Surface Structures (LIPSS), onto

which a square protective grid is superimposed (Fig. 1a). The protective microstructure differs across the surfaces: two mold inserts feature protective grids with pitches of 40 µm and 250 µm, respectively. In contrast, the third insert lacks a protective grid and is therefore referred to as Unprotected (UP). The protective grid exhibits a triangular cross-section, with a width of 10 µm and a height of 2.5 µm (Fig. 1b).

The inserts were mounted in a µ-IM mold, with a part thickness of 2 mm in the textured area, and replicated using a micro-injection molding machine (Micropower 15, Wittmann Battenfeld). The surfaces were replicated in both PP and SEBS, and the processing parameters were optimized for each material using a Design of Experiments (DoE) approach. In particular, the mold temperature (T_{mold}) and melt temperature (T_{melt}) were varied within the ranges recommended by the material supplier (Simax S.p.A.). The injection speed (V_{inj}) was varied between 50 and 200 mm/s, while the packing pressure (p_{hold}) ranged from 100 to 300 bar. For each experimental condition, three repetitions were performed, and ten molding cycles were interposed between the sampling of consecutive DoE points.

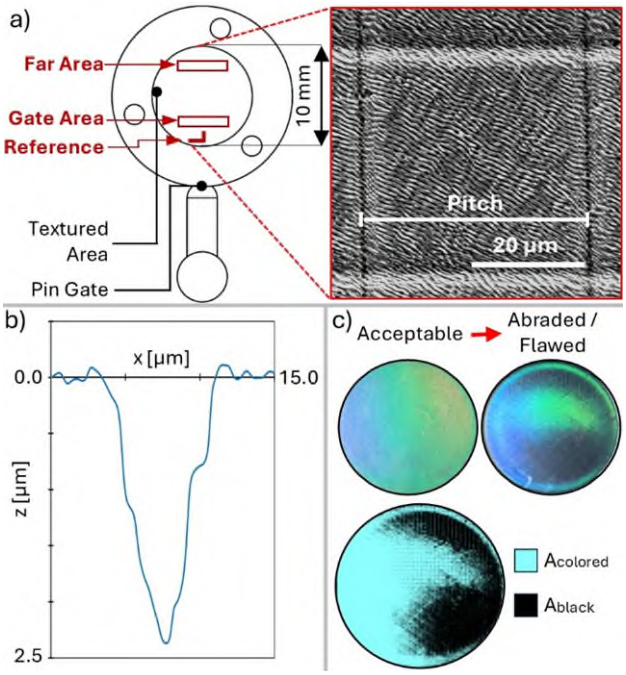

Figure 1. Surface manufacturing and evaluation: (a) schematic of the mold cavity and micrograph of the texture; (b) cross-section of the microfeatures; (c) functionality evaluation.

2.2. Surface geometrical evaluation

Both the mold inserts and the IM samples were geometrically characterized to quantify the degree of feature replication. Quantitative surface characterization was performed using a confocal profilometer equipped with a 100× objective (Plu Neox, Sensofar, SP). Reference features with L-shaped geometry were introduced on the mold surfaces in the gate area to maximize positioning accuracy. Surface scans (1.1 mm × 0.3 mm) were acquired in two different regions of each molded sample: one located 2.5 mm from the reference (*gate area*) and the other at a distance of 7.5 mm from the reference (*far area*) (Fig. 1a). Replication was assessed at micro- and nano-scales due to the hierarchical nature of the surfaces. Replication of the protective microfeatures was quantified by comparing the depth of the microfeatures on the mold inserts (d_{mold}) with the height of the protective mesh on the molded samples (h_{sample}). The micro-scale replication parameter, Q_{micro}, was defined as in eq.1:

$$Q_{micro} = (h_{sample} / d_{mold}) \times 100 \qquad \text{(eq. 1)}$$

Conversely, due to the difficulty of directly measuring LIPSS, sub-micrometric replication was quantified by comparing the roughness parameters Spk and Svk measured on the mold inserts and the molded samples, in accordance with ISO 25178-3. Two replication parameters were therefore defined: one for positive (Q_p, eq.2) and one for negative features (Q_v, eq.3):

$$Q_p = (Spk_{,sample} / Svk_{,mold}) \times 100 \qquad \text{(eq.2)}$$

$$Q_v = (Svk_{,sample} / Spk_{,mold}) \times 100 \qquad \text{(eq.3)}$$

For each acquired scan, the microfeatures were sampled at six locations, while roughness measurements were performed over three distinct areas.

2.3. Abrasion tests

The durability of the µ-IM-fabricated samples was evaluated using a tribometer (MFT-5000, Rtec Instruments), in which a PDMS counterface, consisting of a cylindrical PDMS pad with a diameter of 10 mm and an elastic modulus of 14 MPa, was slid against the textured surfaces. PDMS was selected as the abrasive material as it is considered representative of human touch [11]. A normal load of 5 N was applied, resulting in a nominal contact pressure comparable to that experienced under human finger contact. The abrasive moved sinusoidally over the entire surface at a sliding speed of 25 mm/s. The test was repeated on five different samples for each surface.

Surface functionality (visible structural color) was assessed for all samples that underwent abrasion tests using an optical microscope. The microscope's integrated illumination system ensured consistent lighting during each measurement, enabling the diffraction of white light and structural coloration. Images were captured after each wear test with a 20× objective.

As mechanical loading was applied, areas without structural color gradually appeared on the surface (A_{black}) (Fig. 1c). The size of these regions was quantified through a threshold-based image analysis of the captured pictures. This method allowed monitoring of the surface area that retained functionality under mechanical stress, defined as the colored area ($A_{colored}$) (Fig. 1c).

3. Results and Discussion

3.1. Replication with PP

All process parameters considered were found to be statistically significant in the replication of textures with PP. Process optimization for maximizing the replication accuracy of PP required high values of T_{mold} = 100°C, T_{melt} = 220°C, v_{inj} = 200 mm/s, and p_{hold} = 300 bar. These results are consistent with the literature, where high T_{mold} and T_{melt} reduce the solid skin thickness and material viscosity, respectively, while elevated V_{inj} and p_{hold} promote feature filling [5,6].

Interestingly, the nanoscale replication of LIPSS (Q_p and Q_v) drops sharply on surfaces with microgratings with a pitch of 40 µm (Fig. 2a). This effect is attributed to hesitation and feature-filling dynamics: the injected material initially fills the substrate, then the microcavities, and finally the LIPSS, in an order determined by flow resistance [12]. For surfaces with a 40 µm pitch grid, the high grid density delays LIPSS filling, promoting a thicker solid skin and thus reducing LIPSS replication [11].

Fig. 2b shows the mean replication indices as a function of the distance from the reference position in the gate area, indicating that replication fidelity decreases with increasing distance under identical processing conditions. Q_{micro} is the parameter least affected by distance from the gate, with differences below 5%. In contrast, Q_p and Q_v decrease significantly with increasing distance from the gate, with differences of up to 12.5% and 7.95%, respectively. This behavior is consistent with literature reports attributing it to the distribution of packing pressure in the cavity, highlighting the importance of this parameter for uniform replication of rigid thermoplastics [7].

Results for PP samples are acceptable: Q_{micro} stays above 90%, and variations in Q_p and Q_v don't affect texture functionality.

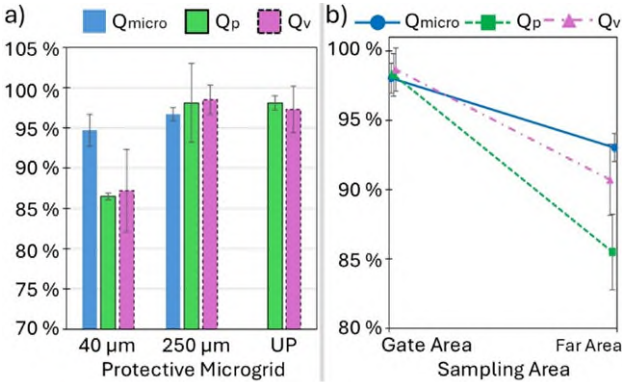

Figure 2. Replication with PP: (a) Surface replication indices; (b) Replication uniformity.

3.2. Replication with SEBS

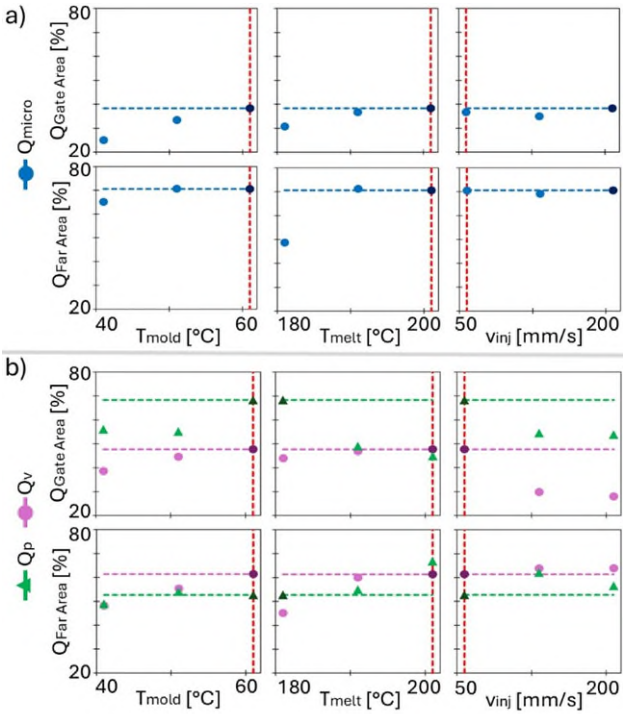

Figure 3. SEBS replication uniformity: a) microfeatures; b) LIPSS.

Process parameter optimization was also performed for SEBS, with the results shown in Fig. 3. Horizontal lines indicate the optimized values, and vertical lines represent the parameters selected for the final replication phase. Analysis of the collected samples revealed that the structural color exhibited a non-uniform distribution across the molded components (Fig. 4a), a phenomenon linked to pronounced heterogeneity in texture replication. Unlike previous reports on rigid thermoplastics and some studies in the literature, ANOVA analysis conducted on the SEBS replication DoE indicates that, although increasing the p_{hold} improves replication, this parameter is statistically negligible compared to the others [5,8].

Fig. 3 also shows that Q_{micro} uniformity is maximized at high injection speeds, whereas the opposite trend is observed for LIPSS replication. In this work, priority was given to replicating sub-micrometric features to preserve surface functionality; therefore, given the minimal effect of injection speed on Q_{micro}, the final samples were molded using v_{inj} = 50mm/s (Fig. 3a). Interestingly, replication near the gate is generally lower than in the region opposite it (Fig. 4a), contrary to observations in µ-IM of rigid thermoplastics [7]. At first glance, and considering the statistically negligible influence of packing pressure, this distribution might be attributed to feature replication during the filling phase. However, this explanation is contradicted by the observed decrease in replication fidelity with increasing injection speed (Fig. 3b). A more plausible explanation is that this behavior arises from greater polymer chain relaxation near the injection point [8,13]. During IM, macromolecules align along the flow direction, with a high degree of alignment at higher shear rates. Upon cooling, macromolecules in the hard phase of SEBS (styrene) become immobilized when their glass-transition temperature (T_g) is reached. In contrast, chains in the soft phase (ethylene-butylene), with a T_g below room temperature, retain some mobility. Consequently, soft-phase macromolecules undergo contraction, the extent of which correlates with their degree of chain alignment [13]. To verify this hypothesis, two injection molding simulations were performed using Moldflow software. In these simulations, the v_{inj} was varied between 50 and 200 mm/s, while the remaining parameters were kept constant at their highest set values to account for the most favorable conditions for replication (T_{mold} = 60°C; T_{melt} = 200°C; p_{hold} = 300 bar) (Fig. 3). The results confirmed the proposed mechanism: in downstream regions, cavity enlargement and the transition from velocity-controlled to pressure-controlled flow reduced shear rates. Higher shear rates in the gate area led to greater macromolecular elongation and relaxation, thereby compromising replication fidelity (Fig. 4a). This region exhibited poor structural color and insufficiently defined nanostructures. Overall, these findings highlight the strong influence of shear rate on macromolecular relaxation and its key role in replication quality, emphasizing the importance of minimizing shear to achieve uniform, high-fidelity surface replication in TPEs (Fig. 4a). The results obtained provide further insight into the complex role of v_{inj} in TPE replication, offering an initial explanation for some findings in the literature [8,9].

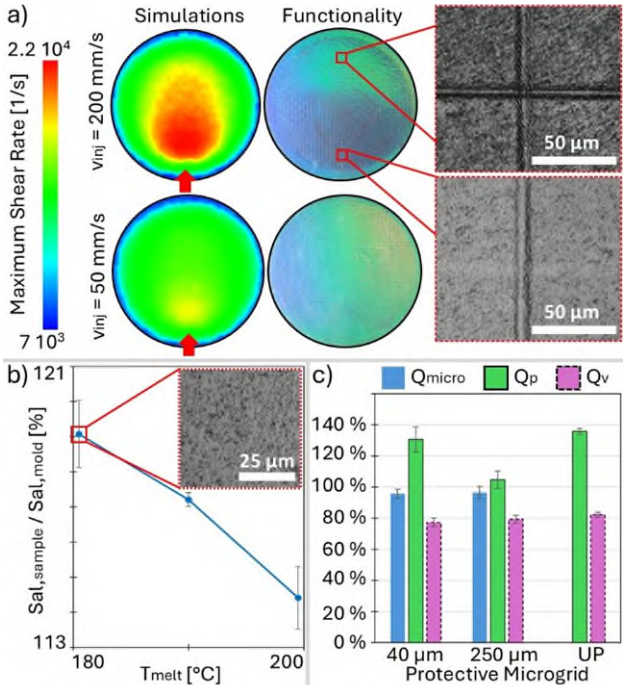

Figure 4. Replication with SEBS: (a) effect of cavity shear rate; (b) nanofeature periodicity in the gate region; (c) final values of the replication metrics.

Except for Q_p, the optimization suggests using high T_{melt} for all processing parameters (Fig. 3). The apparent anomaly in Q_p arises because low T_{melt} promotes surface defects near the gate (Fig. 4b), likely due to relaxation phenomena [8]. Specifically, as T_{melt} decreases, the periodicity of nanostructures increasingly deviates from that of the LIPSS mold inserts. Fig. 4b compares this behavior across different melt temperatures. Analysis using the roughness parameter Sal, sampled according to the

methodology in Section 2.2, shows that lower melt temperatures produce surfaces with nanofeatures significantly exceeding the mold periodicity. Based on this, a higher T_{melt} of 200 °C was chosen for the samples intended for wear testing. These latter observations may partly explain the conflicting results reported in the literature on the effect of T_{melt} [9,10].

Finally, increasing mold temperature consistently improved texture replication; therefore, a high T_{mold} of 90 °C was chosen for subsequent experiments. It is clear that T_{mold} is one of the most critical parameters for the replication of micro- and nanofeatures, even in µ-IM of TPEs [7,8]. The average replication parameter values obtained from the samples are shown in Fig. 4c, highlighting the significant influence of T_{mold}. The replication of the protective grid was excellent in both cases. Interestingly, increasing T_{mold} led to Q_p values exceeding 100%, likely due to adhesion phenomena between the polymer and the mold. In contrast to observations for PP, the variations in replication indices are not correlated with the protective grid pitch. This confirms that, as in TPE replication, the dominant factor is macromolecular relaxation rather than the hesitation effect, and cavity pressure [12,13].

3.3. Abrasion Tests

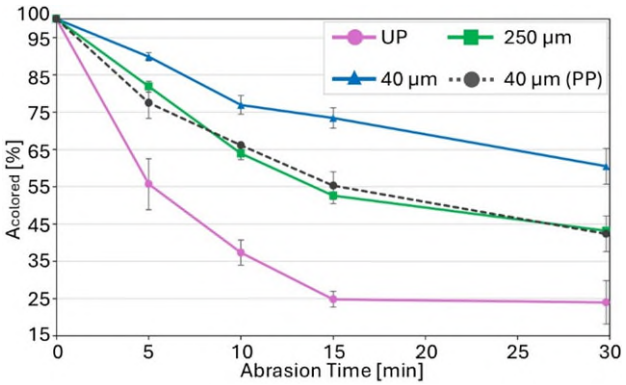

Figure 5. Abrasion test results.

After fabricating all surfaces, abrasion tests were conducted. Results in Figure 5 depict how the residual functional area evolves over abrasion time. The self-protective strategy was tested on SEBS, with similar trends seen in PP [11].

For each time interval, an increase in protective grid density results in a larger residual functional area ($A_{colored}$). The presence of a fine-pitch grid prevents the initial contact between the LIPSS and the PDMS counterface, thereby delaying the onset of abrasion. This behavior is not observed in the 250 µm pitch grid, where the microfeatures primarily reduce the contact pressure between the nanostructures and the abrasive surface [2,11]. The unprotected (UP) surface does not benefit from these mechanisms and consistently exhibits the lowest residual functionalized area among the three configurations.

The self-recovery effect was assessed only for the surface featuring microstructures with a 40 µm pitch. The SEBS surface exhibits enhanced abrasion resistance since it recovers the applied deformations upon removal of the mechanical load [4].

Both strategies enhanced surface durability. The self-recovery approach proved more effective; however, its implementation is technologically more demanding due to TPEs' requirements. Achieving uniform replication in TPEs requires careful control of cavity shear rates and the use of 2K-IM when the final component is a rigid polymer. In contrast, the self-protective strategy does not require material modifications, and the packing pressure mainly governs replication uniformity. This makes the issue readily addressable by adjusting the position of the textured area relative to the injection gate or, when this is not feasible, by employing injection–compression molding [6].

4. Conclusions

The objective of this study was to assess the potential to improve the durability of nanostructured surfaces produced by IM by combining self-protective and self-recovering strategies. To this end, texture replication was first optimized for both rigid thermoplastics and a TPE. In the case of PP, replication accuracy and uniformity were strongly influenced by the packing pressure distribution within the cavity and by hesitation effects during feature filling. Conversely, for TPEs, the replication process was primarily limited by shear-induced macromolecular relaxation in the soft phase, driven by elevated shear rates in the cavity.

Both proposed strategies resulted in enhanced surface durability. The self-protective approach, although less effective, offers greater industrial applicability due to its simplicity and compatibility with conventional injection molding processes. Overall, this work demonstrates different and complementary routes for implementing nanostructured surfaces in real-world applications, where they are expected to withstand repeated human touch and mechanical interaction.

References

[1] Zhang, H., Liu, H., & Zhang, N. (2022). A review of microinjection moulding of polymeric micro devices. *Micromachines*, **13**(9), 1530.

[2] Quan, Y. Y., Chen, Z., Lai, Y., Huang, Z. S., & Li, H. (2021). Recent advances in fabricating durable superhydrophobic surfaces: a review in the aspects of structures and materials. *Materials Chemistry Frontiers*, **5**(4), 1655-1682.

[3] Romano, J. M., Gulcur, M., Garcia-Giron, A., Martinez-Solanas, E., Whiteside, B. R., & Dimov, S. S. (2019). Mechanical durability of hydrophobic surfaces fabricated by injection moulding of laser-induced textures. *Applied Surface Science*, **476**, 850-860.

[4] Mirmohammadi, S. M., Hoshian, S., Jokinen, V. P., & Franssila, S. (2021). Fabrication of elastic, conductive, wear-resistant superhydrophobic composite material. *Scientific reports*, **11**(1), 12646.

[5] Vera, J., Brulez, A. C., Contraires, E., Larochette, M., Trannoy-Orban, N., Pignon, M., ... & Benayoun, S. (2017). Factors influencing microinjection molding replication quality. *Journal of Micromechanics and Microengineering*, **28**(1), 015004.

[6] Calaon, M., Tosello, G., Garnaes, J., & Hansen, H. N. (2017). Injection and injection-compression moulding replication capability for the production of polymer lab-on-a-chip with nano structures. *Journal of Micromechanics and Microengineering*, **27**(10), 105001.

[7] Lucchetta, G., Sorgato, M., Carmignato, S., & Savio, E. (2014). Investigating the technological limits of micro-injection molding in replicating high aspect ratio micro-structured surfaces. *CIRP Annals*, **63**(1), 521-524.

[8] Birkar, S., Mendible, G., Park, J. G., Mead, J. L., Johnston, S. P., & Barry, C. M. (2016). Effect of feature spacing when injection molding parts with microstructured surfaces. *Polymer Engineering & Science*, **56**(12), 1330-1338.

[9] Stormonth-Darling, J. M., Saeed, A., Reynolds, P. M., & Gadegaard, N. (2016). Injection Molding Micro-and Nanostructures in Thermoplastic Elastomers. *Macromolecular materials and engineering*, **301**(8), 964-971.

[10] Vega, M. D. J., Mead, J., & Barry, C. (2016). Injection molding microstructured substrates from rubber-containing polymers. *In AIP Conference Proceedings* (Vol. 1779, No. 1, p. 020012). AIP Publishing LLC.

[11] Sorgato, M., Baruffa, G., Oubellaouch, K., Zaniboni, G., & Lucchetta, G. (2025). A novel method for high-volume manufacturing of self-protective plastic surfaces to ensure durable anti-counterfeiting functionality. *CIRP Annals*.

[12] Yang, C., Huang, H. X., Castro, J. M., & Yi, A. Y. (2011). Replication characterization in injection molding of microfeatures with high aspect ratio: Influence of layout and shape factor. *Polymer Engineering & Science*, **51**(5), 959-968.

[13] Lu, J., Zhang, H., Chen, Y., Ge, Y., & Liu, T. (2022). Effect of chain relaxation on the shrinkage behavior of TPEE foams fabricated with supercritical CO2. *Polymer*, **256**, 125262.